Extended Circular Dichroism Measurements Using Synchrotron Radiation Show That the Assembly of Clathrin Coats Requires No Change in Secondary Structure†

David T. Clarke and Gareth R. Jones*

Synchrotron Radiation Department, CLRC Daresbury Laboratory, Warrington WA4 4AD, U.K.

Received March 16, 1999; Revised Manuscript Received June 1, 1999

ABSTRACT: A number of models have been proposed for the assembly of clathrin triskelia into coats. However, little is known of the effects of assembly on triskelion structure. A more detailed knowledge of the way in which assembly affects triskelion structure would be valuable for assessing the relative merits of the proposed models. The development of a vacuum-ultraviolet circular dichroism (CD) instrument that uses synchrotron radiation as a light source has allowed us to extend the range of CD measurements to shorter wavelengths. This has greatly increased signal quality even for highly scattering samples. Also, we have improved CD data analysis to provide standard deviations for calculated secondary structure content. These developments have increased the precision of CD analysis beyond what has been thus far possible. Using these developments, we have determined the secondary structure content of all components of coat protein, under both assembly and dissociating conditions. The assembly of coats does not incur any change in secondary structure content, but a 10% loss of triskelion helical content accompanies assembly in the absence of AP-2. We conclude that coat assembly requires no detectable reorganization of triskelion structure. Our result indicates that AP-2 stabilizes helical structure in the triskelion, and we propose that this increases triskelion rigidity, restricting the range of coat sizes.

The structure of clathrin coats has been studied extensively (*1*−*4*), but the nature and sequence of events leading to coat assembly are not yet understood. In particular, little is known about the structural basis for regulation of coat assembly by the assembly polypeptides, APs.[1] Coat protein is composed of triskelia, which are three-legged structures consisting of three 190 kDa heavy chains, three light chains of 25−29 kDa (*5*), and the APs (*6*). The AP associated with the plasma membrane is designated AP-2 (*6*). Triskelia can be assembled, in vitro, to form empty structures that are similar in appearance to the coats of coated vesicles (*1*), and are denominated coats in the presence of APs and cages in their absence (*2*).

The clathrin heavy chain has a domain structure, consisting of the globular terminal domain and elongated distal and proximal domains (*7*). The three legs of the triskelion are connected at the "trimerization site", situated at the hub of the proximal domain (*8*). Enzymatic digestion of the triskelion cleaves the terminal domain (52 kDa) from the hub (110 kDa), with the loss of a linker region (*9*). It has been reported that hubs also form cages (*10*). The C-terminal third of the heavy chain has been obtained by expression in bacteria (*8*). This polypeptide is also referred to as the "hub", but its molecular mass of 68 kDa makes it considerably smaller than hubs prepared by enzymatic digestion; consequently, it forms polymorphic assemblies.

Little is known of the submolecular changes that occur on assembly. However, some modifications of the triskelion leg structure must occur to accommodate the excess length of the distal domain compared to the proximal domain (*2*). Models that have been proposed to account for this include intertwining of the distal domains of the legs (*2*), "scrolling" of the distal and terminal domain to vary leg length (*11*), and flexing of a hinge region to project the terminal domain into the coat interior (*4*). The latter model has recently gained support as the result of a 21 Å resolution cryoelectron microscopy study of coats, which shows side-by-side packing of the legs with the distal domains pointing inward (*3*).

AP-2 plays a major role in mediating the assembly process. Populations of plasma membrane-derived coats have a relatively uniform diameter of 65 nm (*6*), but cages have a broader size distribution, ranging to 112 nm (*12*, *13*), or even 120 nm, in diameter (*11*). Coats are stable under a much wider range of conditions than cages, and are more resistant to disassociation by elevated pH (*1*). Little is known about the structural basis for this regulation of coat assembly by AP-2. Electron micrographs show the triskelion to be a rigid structure (*11*), and therefore, the cage size must be determined by the pucker angle of the triskelion (*14*). The pucker angle is defined as the solid angle between the trimer legs at the hub; a larger angle will therefore result in cages with greater diameters, and it has been proposed that AP-2 binding, in some way, causes the formation of smaller structures by decreasing this angle. A knowledge of how the secondary structure of the triskelion changes during assembly in the presence and absence of AP-2 would indicate

† The work was supported by the Biotechnology and Biological Sciences Research Council through the provision of SRS beam time.

* Corresponding author. Telephone: +44 (0)1925 603539. Fax: +44 (0)1925 603124. E-mail: g.r.jones@dl.ac.uk.

[1] Abbreviations: AP, assembly polypeptide; CD, circular dichroism; SR, synchrotron radiation; NMR, nuclear magnetic resonance; HC, heavy chain; LC, light chain; TD, terminal domain; PD, proximal domain; CIDS, circular intensity differential scattering; PEM, photoelastic modulator.

10.1021/bi990604j CCC: $18.00
Published on Web 07/23/1999

how AP-2 might modulate assembly and provide new evidence to distinguish between the above structural models that account for the mismatch in the length of the distal leg region.

Far-ultraviolet circular dichroism (CD) is a most convenient technique for the investigation of secondary structure of protein in solution, but has not, thus far, been applied effectively to any protein self-assembly system. Attempts have been made to measure changes in the CD spectrum that accompany assembly in, for example, tobacco mosaic virus coat protein (*15*), the coat protein of the filamentous bacteriophage fd (*16*), and the f1 phage coat protein (*17*). However, the limited spectral range of conventional instruments and the distortions caused by circular intensity differential scattering (CIDS) in turbid samples (*18*) have prevented structural analysis. These limitations have now been largely overcome by an instrument that minimizes the detrimental effect of solution turbidity by the close positioning of sample and detector, and the use of synchrotron radiation (SR) as a light source which enables the collection of CD data to 175 nm. Extending the wavelength range of CD spectra greatly improves the accuracy of secondary structure determinations, usually to within an average of 3% of that obtained from X-ray crystallography (*19*).

We have used SRCD to determine the secondary structure content with high precision of all the components of coat protein, under assembly and dissociating conditions. Coat protein exhibits no change in secondary structure content on assembly. In contrast, isolated triskelia and hubs exhibit a loss of helical content on assembly. Stopped-flow SRCD shows that the structural changes associated with cage formation occur within 1 ms of the pH jump that initiates assembly. Our results are consistent with a model for assembly that does not require the intertwining of triskelia.

MATERIALS AND METHODS

Protein Preparation. Clathrin coat protein was isolated from porcine brains using a modified version of the method of Keen et al. (*1*). Clathrin was separated from its assembly polypeptides by dialysis against 1.0 M Tris-HCl buffer (pH 7.0) containing 0.2 mM dithiothreitol, 0.5 mM phenylmethanesulfonyl fluoride (PMSF), and 0.02% NaN_3 (buffer B), prior to elution on a Sepharose CL-4B column (Pharmacia) that had been equilibrated with the same buffer. AP-2 was also obtained from this fractionation (*14*). Light chains were isolated using the method of Winkler and Stanley (*20*). Fragments of clathrin were prepared by the digestion of coat protein with subtilisin BPN′ at a ratio of 1 unit/25 mg of protein, in 0.1 M Na MES buffer (pH 6.2) containing 1.0 mM EGTA, 0.5 mM $MgCl_2$, and 0.02% NaN_3 (buffer A), at 25 °C for 90 min. Enzyme activity was determined by the rate of release of tyrosine from casein, monitored using Folin's reagent (1 unit of enzyme hydrolyzes casein to produce a color equivalent to 1.0 μmol of tyrosine per minute at pH 7.5 and 37 °C). A Superose 12 FPLC column (Pharmacia) was used to fractionate the digestate into hubs and terminal domains. All buffers and salts used for this work were of analytical grade. The digest samples were characterized by SDS−polyacrylamide gel electrophoresis, and electrospray mass spectrometry which was undertaken at the Michael Barber Centre for Mass Spectrometry, UMIST, UK (VG, Quattro Tandem Quadrupole). The proportion of AP-2 in the preparations was determined by integrating the protein absorption peaks following elution of coat protein on a Superose 6 FPLC column in buffer B. Sample concentrations were determined by absorbance at 280 nm. Where light scattering from assembled samples interfered with the concentration determination, the samples were prepared in the disassembled state and dialyzed under assembly conditions. The BCA method (*21*) was used to correct for any concentration changes that might have occurred as the result of dialysis.

Circular Dichroism. CD spectra were collected on experimental station 3.1 of the CLRC Daresbury Laboratory's Synchrotron Radiation Source (SRS). This facility comprises a vacuum-ultraviolet 1 m Seya-Namioka monochromator, which provides a high flux of linearly polarized light in the wavelength range from 120 to 300 nm. The linear polarization is converted to circular polarization, switched between right and left at a frequency of 50 kHz, using a photoelastic modulator (PEM) (*22*). The CD signal is a 50 kHz AC component that is superimposed on a DC level. The AC component is separated from the DC, and amplified. The voltage supplied to the photomultiplier serves to maintain a constant DC level, irrespective of the sample absorbance as a function of wavelength, and synchrotron beam current. The AC signal is then processed in a lock-in amplifier, the phase reference being supplied from the PEM. The lock-in amplifier isolates the CD signal from noise components at other frequencies, or out-of-phase noise at 50 kHz. A Fused silica cell with a 100 μm path length was used with the sample concentration of 1 mg/mL. The sample chamber was purged with dry nitrogen to remove oxygen from the optical path. The sample cells were positioned 2 mm from the entrance window of the photomultiplier to minimize errors associated with light scattering from turbid samples. Spectra were collected for all coat protein components under assembly conditions [10 mM phosphate (pH 6.0)] and disassembly conditions [10 mM phosphate (pH 8.0)], all prepared by dialysis from the same stock solution in buffer B. Protein concentrations were checked after dialysis using the BCA method. Spectra were also recorded for coat protein, pure triskelia, and AP-2 in 1.0 M Tris buffer (pH 7.0), conditions which we know from molecular exclusion chromatography cause complete disassembly of coats and the release of AP-2 from triskelia. The spectra were buffer subtracted, and scaled to molar ellipticity using the CD spectrum of a 1 mg/mL solution of (+)-10-camphorsulfonic acid. Averages of three spectra from individual samples were used for analysis. Analysis of secondary structure content was undertaken with a modified version of the program Selcon (*23*), using a set of basis spectra collected with station 3.1 over the wavelength range of 168−260 nm. The program was enhanced to provide standard deviations for calculated secondary structure content. Standard deviations in analysis were calculated from the covariance matrixes for the basis set components and basis set spectra, for each choice of a basis set and a number of singular values. Standard deviations obtained by this method are in close agreement with those obtained for test data from proteins of known secondary structure (D. T. Clarke, R. Denny, and G. R. Jones, unpublished data).

Secondary structure content of polypeptide regions not directly determined by SRCD was calculated by subtracting

the fractional secondary structure content of the other regions from that of the entire protein. The fraction of a structure type in a region is given by

$$pD = A - (pB + pC)$$

where p is the fraction of each polypeptide region by mass, A is the percentage of the structure type in the whole structure, B and C are the percentages in known domains of the structure, and D is the percentage in the unknown domain.

The degree of light scattering from the samples was assessed by apparent absorption at 220 nm, after subtraction of the true absorption from the proteins, measured under disassembly conditions.

Stopped-flow measurements were performed on SRS station 13.1b using a specially constructed stopped-flow device with a dead time of 2.3 ms, fitted with a 0.5 mm path length cell with fused silica windows. The principle of operation, using a photoelastic modulator to convert the horizontally polarized synchrotron light to circularly polarized light, was the same as for scanning measurements. For stopped-flow experiments, a commercially available data acquisition system was used (Applied Photophysics SX-17MV). The time resolution was set at 2 ms. Measurements were recorded at 210 nm, where the maximum change in CD signal was observed on cage assembly.

X-ray Solution Scattering. X-ray solution scattering measurements were performed on SRS station 2.1 (*24*). Samples at a concentration of 1 mg/mL were placed in a 1 mm path length cell fitted with 25 μm ruby mica windows, and exposed to the 1.54 Å wavelength X-ray beam. A camera length of 6 m was used, giving a scattering vector range in reciprocal space ($S = 2 \sin \theta/\lambda$) from 0.001 to 0.01 Å^{-1}. A multiwire quadrant detector with associated electronics (*25*) was used for data collection.

Cryoelectron Microscopy. Cryoelectron microscopy was performed on a Philips EM430 transmission electron microscope, operating at an accelerating voltage of 100 kV, and fitted with an anticontaminator (Gatan 651N). Protein solutions (0.05 mg/mL) were applied to holey carbon grids, which were then blotted and fast-frozen by plunging into liquefied ethane (*26*). The grids were transferred to the microscope using a cryotransfer device (Gatan 626) and micrographs recorded using a low-dose imaging regime. Electron micrograph films were then densitometered at a resolution of 10 μm using a flat-bed microdensitometer (JL Automation MDM6). The images were processed using BSL (Synchrotron Radiation Source Program Library, Daresbury Laboratory) and AVS (AVS/Uniras Ltd.).

RESULTS

Characterization of the Protein Preparations. Preparations of coat protein were fully characterized by SDS−PAGE, molecular exclusion chromatography, electrospray mass spectrometry, cryotransmission electron microscopy, and X-ray solution scattering, as an essential prerequisite for assessing the purity and assembly competence of the protein. The polypeptide composition of our preparations is entirely consistent with the familiar pattern reported many times (Figure 1). The digest components consisted of the hub region with the light chains intact, and the terminal domain. Electrospray mass spectrometry on the proximal and terminal

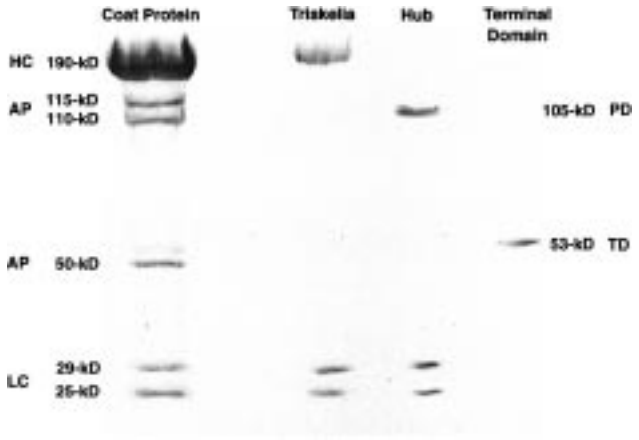

FIGURE 1: SDS−polyacrylamide gel electrophoresis of coat protein and its components (HC, heavy chain; LC, light chain; AP, assembly polypeptide; PD, proximal domain; and TD, terminal domain).

domains gave molecular masses of 105.1 and 53.3 kDa, respectively. AP-2 constituted 30% of the mass of the coat protein in our preparations.

Confirmation of the sizes of assemblies formed by coat protein, triskelia, and hubs was obtained from cryotransmission electron microscopy (Figure 2). Table 1 shows that coat protein forms structures 65 nm in diameter, the small percentage of larger structures corresponding to the percentage of contamination by AP-1. Purified triskelia and hubs form a bimodal distribution of 65 and 112 nm structures. This confirms that the presence of AP-2 influences coat size, as proposed elsewhere. Micrographs show that the percentage of protein assembled into cages is 80% and into hub cages is 62% when compared with coats at a protein concentration of 0.05 mg/mL. X-ray solution scattering was used to confirm the degree and proportion of cage assembly at the protein concentration used for the SRCD measurements (1 mg/mL). These parameters are derived from the relative intensity of the central scatter region (at low scattering vector) and the prominence of the subsidiary maximum at 0.004 Å^{-1}, when compared with highly concentrated preparations. These measurements show that coat protein, triskelia, and hubs all form a similar proportion of well-defined coats and cages under assembly conditions (Figure 3).

SRCD Spectra. SRCD measurements were taken on all components of coat protein, under assembly and disassembly conditions (Figure 4). The excellent quality of the spectral data enables secondary structural analysis to high precision, as indicated by the calculated standard deviations (Table 2). Coat protein (containing AP-2) exhibited no significant change in secondary structure content between assembly and disassembly conditions, but in the absence of AP-2, triskelia and hubs exhibited a significant 10 and 7% decrease in helical content in assembly conditions, respectively. In the presence of dissociated AP-2 [1.0 M Tris (pH 7)], the triskelion helical content approximates that of dissociated triskelia, confirming that binding of AP-2 is required to regulate the triskelion secondary structure.

Coat protein is a complex mixture of large proteins, and therefore, the presence of a high proportion of polypeptide with unchanging secondary structure content would diminish the effect of a change in the secondary structure of the

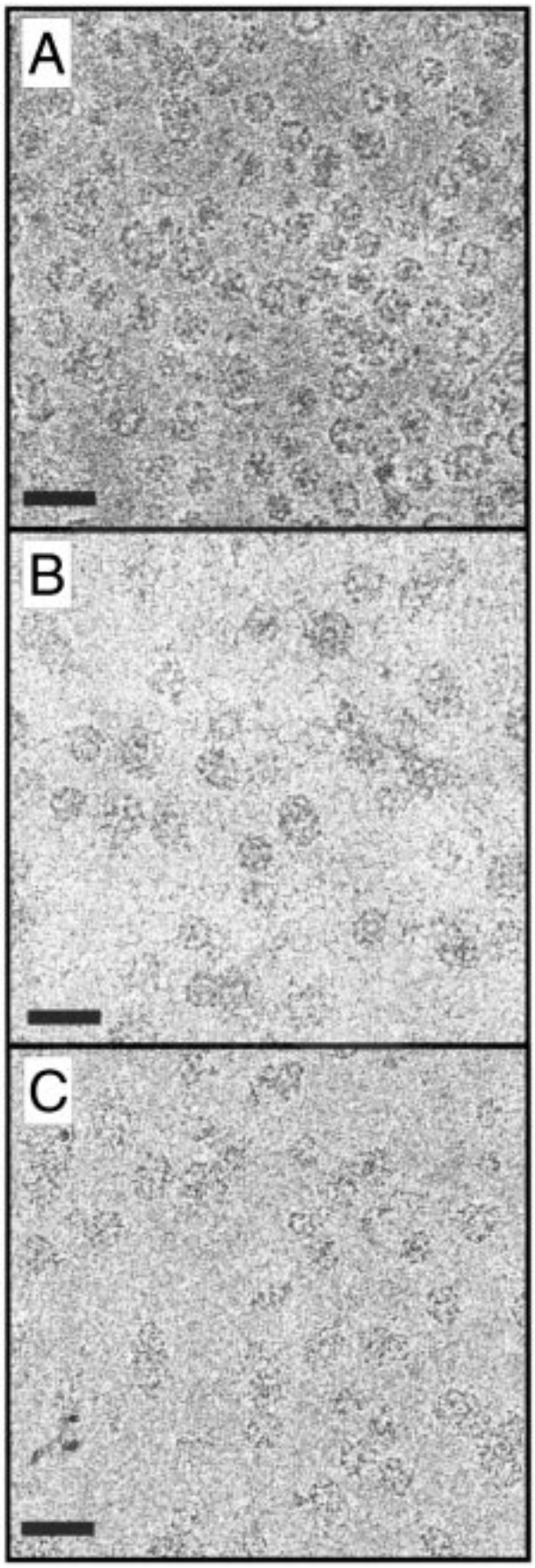

FIGURE 2: Cryoelectron micrographs of (A) coat protein, (B) triskelia, and (C) hubs under assembly conditions, with a protein concentration of 0.05 mg/mL (bar is 200 nm).

Table 1: Proportions of Large and Small Coats or Cages Formed from Coat Protein, Triskelia, and Hubs

	coat protein	triskelia	hubs
% small (<85 nm)	92.7	49.8	56.2
% large (>85 nm)	7.3	51.2	43.8
no. of structures counted	326	261	222

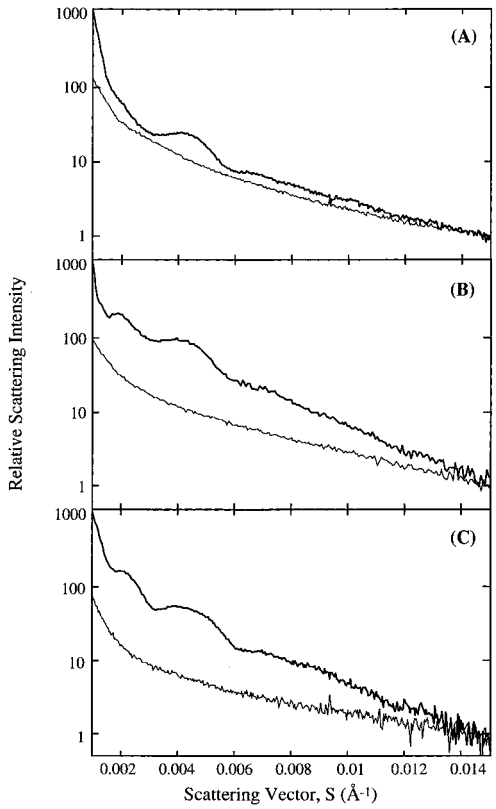

FIGURE 3: X-ray solution scattering patterns of (A) coat protein, (B) triskelia, and (C) hubs under assembly (thick line) and disassembly (fine line) conditions, with a protein concentration of 1 mg/mL.

triskelion. To account for this, we have calculated the total secondary structure change that would be observed in coat protein if its triskelia changed in a similar way on assembly as in cages. This would result in a decrease in helical content of 7%, a change that would be easy to detect. However, no significant change is observed. Also, the complexity of the coat protein system makes it inconceivable that changes in the secondary structure of all of the components would result in no net change. In addition, we show that the secondary structure content of both AP-2 and light chains is pH-independent (Table 2, v and vi). We therefore affirm that the secondary structure of the triskelion in coat protein does not change on assembly (Table 2, vii). Assembly therefore could involve only minor changes, such as flexing of a small hinge region.

CD studies of self-assembly proteins have hitherto been hindered by the presence of scattering artifacts, for example, in assembled f1 bacteriophage (*17*). We can eliminate the possibility of scattering artifacts in our data on several grounds. First, the magnitudes of the CD bands at 193 and 210 nm are not significantly depressed with respect to the band at 223 nm. Second, the signal-to-noise ratio at 190 nm is high. Also, all the CD spectra shown in Figure 4 return to a zero baseline level at or before 260 nm. Finally, there is

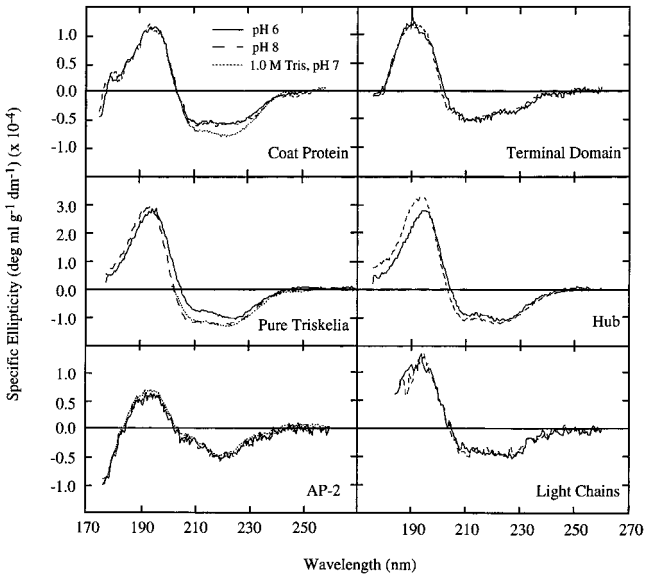

FIGURE 4: Circular dichroism spectra of components of coat protein in 10 mM phosphate at pH 6 (solid line), 10 mM phosphate at pH 8 (dashed line), and 1.0 M Tris-HCl at pH 7 (dotted line), with a protein concentration of 1 mg/mL.

no observable difference for coat protein between assembly and disassembly conditions, although this shows the highest change in turbidity (apparent absorption under assembly conditions was 2.07 for coat protein, 1.32 for triskelia, and 0.87 for hubs). Taken together, these findings show that the data are not affected by absorption flattening, light scattering, or CIDS (*18*, *27*).

Stopped-Flow SRCD. Stopped-flow SRCD measurements show that there is no observable change in the secondary structure of triskelia during assembly, with the magnitude of the CD signal being equivalent to that measured for assembled cages (Figure 5). This shows that the change in secondary structure occurs well within the dead time of the stopped-flow apparatus (1 ms). Cage assembly is, however, known to occur over a period of several seconds to several hours (*28*). This leads us to the conclusion that the secondary structure changes occur at the early stages of assembly, and are caused directly by the change in pH, rather being a consequence of the assembly process, such as leg intertwining or scrolling.

DISCUSSION

The data presented clearly show the superiority of synchrotron radiation as a light source for CD. The high signal-to-noise ratios and extended wavelength range have allowed secondary structure content to be determined with both high accuracy and precision. Also, the instrumental geometry, combined with high photon flux, has enabled the collection of CD spectra from turbid samples, which are free from scattering artifacts compounded by high noise levels. We expect the instrument to find many uses in the application of CD for turbid samples, as may be encountered with large macromolecular assemblies and membrane−protein complexes. The high flux of SR is also very well-suited to time-resolved stopped-flow CD. High photon fluxes allow the collection of noise-free data from small sample quantities, over a wider wavelength range than can be achieved with conventional instruments.

Table 2: Percentages of Secondary Structure Types of Components of Coat Protein[a]

	sample	α	β	turns	"random"
i	coat protein at pH 6	39 (0.60)	23 (1.16)	14 (0.63)	24 (1.23)
	coat protein at pH 8	39 (0.43)	20 (1.06)	16 (0.56)	25 (1.23)
	coat protein and 1.0 M Tris*	48 (0.93)	12 (2.86)	12 (1.10)	28 (2.53)
ii	pure triskelia at pH 6	52 (0.83)	12 (2.40)	13 (1.76)	23 (3.36)
	pure triskelia at pH 8	62 (0.53)	4 (1.26)	7 (0.93)	27 (2.40)
	pure triskelia at pH 8*	62 (0.96)	8 (3.70)	12 (2.20)	18 (4.23)
	pure triskelia with 1.0 M Tris*	62 (1.26)	11 (3.23)	14 (2.36)	13 (3.06)
iii	hubs at pH 6	70 (0.70)	13 (2.83)	13 (1.56)	4 (4.33)
	hubs at pH 8	77 (1.06)	1 (1.53)	14 (1.80)	8 (2.80)
	hub fragment at pH 8[b]	75	0	12	13
iv	terminal domains at pH 6	33 (0.60)	20 (1.30)	20 (0.76)	27 (1.10)
	terminal domains at pH 8	33 (0.70)	21 (1.20)	21 (0.70)	25 (1.00)
v	light chains at pH 6	34 (1.06)	20 (1.43)	18 (0.86)	28 (2.26)
	light chains at pH 8	34 (1.00)	19 (1.33)	20 (0.76)	27 (1.96)
vi	AP-2 at pH 6	21 (0.33)	23 (1.03)	22 (0.33)	34 (0.40)
	AP-2 at pH 8	21 (0.76)	23 (1.83)	21 (0.63)	35 (2.00)
	AP-2 with 1.0 M Tris*	22 (0.86)	22 (2.16)	21 (1.00)	35 (2.26)
vii	triskelia in coat protein at pH 6	51	21	10	19
	triskelia in coat protein at pH 8	51	20	11	19
	triskelia in coat protein with 1.0 M Tris*	62	2	3	25

[a] Data for i−vi are from analysis of SRCD data. Data for vii were calculated from subtraction of the proportional percentage structure content of AP-2 from that of the coat protein. Spectra were analyzed over the wavelength range of 175−260 nm, except those marked with an asterisk, which were restricted to a range of 202−260 nm, so that a comparison could be made with those measurements performed in 1 M Tris buffer. Measurements over this restricted wavelength range are less accurate, and total secondary structure percentages deviate from 100 in some cases. Standard deviations are shown in parentheses, and were determined from the Selcon fitting parameters, as described in Materials and Methods. [b] The secondary structure content for the hub fragment (residues 1210−1516) was dervied from the published crystal structure, obtained at pH 8 (*31*). The secondary structure content is very similar to that obtained from CD for the entire hub, indicating that the structures of the crystallized and uncrystallized portions of the hub are similar. This supports the model in which the entire filamentous portion of the leg consists of a coil of α-helices.

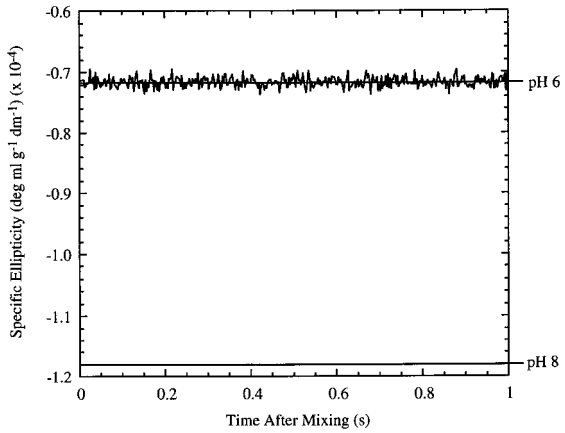

FIGURE 5: Stopped-flow circular dichroism measurement at 210 nm on triskelia following a rapid change from disassembly to assembly conditions (pH 8 to 6). The lines correspond to the steady-state CD signal at 210 nm for the two pH values.

Our data show that no significant changes in clathrin secondary structure are required for the assembly of coats. This finding discounts models of assembly that involve large changes in triskelion structure, such as intertwining of the

distal domains (*2*), or scrolling of the terminal domain (*11*). This is consistent with the model proposed from cryoelectron microscopy (*3*, *4*), in which the legs lie parallel to each other and the excess length is accommodated by the flexing of a hinge to project the terminal domains into the coat. The flexing of a hinge to accommodate assembly is not unique in self-assembly systems, and would not be expected to involve large changes in secondary structure. For example, the membrane-mediated assembly of bacteriophage Pf1 coat protein is initiated by a 90° bend of its hinge region with no significant change in secondary structure that can be detected by NMR spectroscopy (*29*).

It is unlikely that the assembly of cages occurs by a mechanism significantly different from that of coats, because of the similarity of the assemblies that are formed. The changes in secondary structure observed are induced by a change in pH, and are not expected to occur in vivo, where AP-2 is presumably always present. We conclude that AP-2 has a stabilizing effect on the secondary structure of the triskelion. It appears to prevent decreases in triskelion helix content that occur with a decrease in pH in the absence of AP-2, thus maintaining triskelion rigidity, as helices are the most rigid of secondary structure components (ignoring tertiary contacts). Increased triskelion flexibility in the absence of AP-2 has previously been observed by electron microscopy (*30*). Increased triskelion flexibility would be expected to increase the range of coat sizes, so a rigidifying effect of AP-2 might account for its restricting effect on coat size distribution.

ACKNOWLEDGMENT

Thanks are due to Mr. Stephen Hill, Mr. Tony Hinde, Mr. Malcolm Miller, Mr. Nigel Rimmer, Mr. James Sheldon, and Mr. Alan Whitehead for construction of parts of the stopped-flow apparatus. We also thank Dr. Richard Denny for his work on the CD analysis program, Selcon.

REFERENCES

1. Keen, J. H., Willingham, M. C., and Pastan, I. H. (1979) *Cell 16*, 303−312.
2. Crowther, R. A., and Pearse, B. M. F. (1981) *J. Cell Biol. 91*, 790−797.
3. Smith, C. J., Grigorieff, N., and Pearse, B. M. F. (1998) *EMBO J. 17*, 4943−4953.
4. Vigers, G. P. A., Crowther, R. A., and Pearse, B. M. F. (1986) *EMBO J. 5*, 2079−2085.
5. Brodsky, F. M., Hill, B. L., Acton, S. L., Näthke, I., Wong, D. H., Ponnambalam, S., and Parham, P. (1991) *Trends Biochem. Sci. 16*, 208−213.
6. Pearse, B. M. F., and Robinson, M. S. (1984) *EMBO J. 3*, 1951−1957.
7. Kirchhausen, T., Harrison, S. C., Ping Chow, E., Mattaliano, R. J., Ramachandran, K. L., Smart, J., and Brosius, J. (1987) *Proc. Natl. Acad. Sci. U.S.A. 84*, 8805−8809.
8. Liu, S.-H., Wong, M. L., Craik, C. S., and Brodsky, F. M. (1995) *Cell 83*, 257−267.
9. Kirchhausen, T., and Harrison, S. C. (1984) *J. Cell Biol. 99*, 1725−1734.
10. Schmid, S. L., Matsumoto, A. K., and Rothman, J. E. (1982) *Proc. Natl. Acad. Sci. U.S.A. 79*, 91−95.
11. Heuser, J. E., and Kirchhausen, T. (1985) *J. Ultrastruct. Res. 92*, 1−27.
12. Nandi, P. K., Pretorius, H. T., Lippoldt, R. E., Johnson, M. L., and Edelhoch, H. (1980) *Biochemistry 19*, 5917−5921.
13. Zaremba, S., and Keen, J. H. (1983) *J. Cell Biol. 97*, 1339−1347.
14. Keen, J. H. (1987) *J. Cell Biol. 105*, 1989−1998.
15. Schubert, D., and Krafczyk, B. (1969) *Biochim. Biophys. Acta 188*, 155−160.
16. Roberts, L. M., and Dunker, A. K. (1993) *Biochemistry 32*, 10479−10484.
17. Nozaki, Y., Chamberlain, B. K., Webster, R. E., and Tanford, C. (1976) *Nature 259*, 335−338.
18. Tinoco, I., Jr., Mickols, W., Maestre, M. F., and Bustamante, C. (1987) *Annu. Rev. Biophys. Biophys. Chem. 16*, 319−349.
19. Toumadje, A., Alcorn, S. W., and Johnson, W. C., Jr. (1992) *Anal. Biochem. 200*, 321−331.
20. Winkler, F., and Stanley, K. K. (1983) *EMBO J. 2*, 1393−1400.
21. Smith, P. K., Krohn, R. I., Hermanson, G. T., Mallia, A. K., Gartner, F. H., Provenzano, M. D., Fujimoto, E. K., Goeke, N. M., Olson, B. J., and Klenk, D. C. (1985) *Anal. Biochem. 150*, 76−85.
22. Kemp, J. C. (1969) *J. Opt. Soc. Am. 59*, 950−954.
23. Sreerama, N., and Woody, R. W. (1993) *Anal. Biochem. 209*, 32−44.
24. Towns-Andrews, E., Berry, A., Bordas, J., Mant, G. R., Murray, P. K., Roberts, K., Sumner, I., Worgan, J. S., Lewis, R., and Gabriel, A. (1989) *Rev. Sci. Instrum. 60*, 2346−2349.
25. Worgan, J. S., Lewis, R., Fore, N. S., Sumner, I. L., Berry, A., Parker, B., D'Annunzio, F., Martin-Fernandez, M. L., Towns-Andrews, E., Harries, J. E., Mant, G. R., Diakun, G. P., and Bordas, J. (1990) *Nucl. Instrum. Methods Phys. Res. A291*, 447−454.
26. Dubochet, J., Adrian, M., Chang, J. J., Homo, J. C., Lepault, J., McDowall, A. W., and Schultz, P. Q. (1988) *Q. Rev. Biophys. 21*, 129−228.
27. Swords, N. A., and Wallace, B. A. (1993) *Biochem. J. 289*, 215−219.
28. Van Jaarsveld, P. P., Nandi, P. K., Lippoldt, R. E., Saroff, H., and Edelhoch, H. (1981) *Biochemistry 20*, 4129−4135.
29. Nambudripad, R., Stark, W., Opella, S. J., and Makowski, L. (1991) *Science 252*, 1305−1308.
30. Kocsis, E., Trus, B. L., Steer, C. J., Bisher, M. E., and Steven, A. C. (1991) *J. Struct. Biol. 107*, 6−14.
31. Ybe, J. A., Brodsky, F. M., Hofmann, K., Lin, K., Liu, S.-H., Chen, L., Earnest, T. N., Fletterick, R. J., and Hwang, P. K. (1999) *Nature 399*, 371−375.

BI990604J